Physical Layer Performance for Coexistence of Bluetooth and IEEE 802.11b

Amir Soltanian and Robert E. Van Dyck
National Institute of Standards and Technology
Gaithersburg, MD 20899
{amirs, vandyck}@antd.nist.gov

Abstract - Simulations are employed to evaluate the physical layer performance of Bluetooth and IEEE 802.11b receivers, mainly but not exclusively, in interference-limited environments. For Bluetooth, a limiter-discriminator with post-detection integrate and dump filtering (LDI) is used. Bit error rate curves are obtained for co-channel and adjacent channel(s) interference in AWGN and flat fading channels. The interference in this case may be a different Bluetooth piconet or an 802.11b transmitter. For 802.11b, differentially coherent 1 Mbit/sec and coherent 11 Mbits/sec receivers are studied with Bluetooth interference, again obtaining BER curves for both AWGN and fading channels. Finally, the LDI is replaced with a coherent Viterbi receiver, and the performance in the interference-limited environment is measured.

1 Introduction

With the coming deployment of Bluetooth wireless personal area networks (WPANs) [1] in the 2.4-GHz ISM band, there is a growing concern about coexistence with other existing systems, especially the IEEE 802.11b wireless local area network (WLAN). The Bluetooth system employs frequency hopping to mitigate the effect of interference and fading channel impairments. A direct sequence spread spectrum (DSSS) 802.11b system occupies approximately 22 MHz in the same band. Therefore, the Bluetooth system will consistently hop into the 802.11b spectrum, causing interference to both. Additionally, the frequency hopping pattern for different Bluetooth networks, called piconets, are not coordinated, so that multiple piconets operating in the same geographic area will interfere with each other.

This paper addresses the coexistence issue by applying baseband models for the physical layers of the two systems. Using appropriate channel models based on recent measurements, we determine the performance degradation in a prototype environment.

The Bluetooth system operates at a channel bit rate of 1 Mbit/sec [2]. The modulation is Gaussian frequency shift keying (GFSK) with a nominal modulation index of $h_f = 0.32$ and a normalized bandwidth of $B_bT = 0.5$, where B_b is the 3 dB Bandwidth of the transmitter's Gaussian low pass filter, and T is the bit period. The Bluetooth radio employs a frequency hopping scheme in which the carrier frequency is changed on a packet by packet basis. There are up to 79 different channels each with 1 MHz separation. The primary communication range is 10 m, but it can be extended up to 100 m. The entire structure of the simulated system is presented in Fig. 1. It includes the transmitter, the channel noise, the receiver and the interference source. The interference source can be selected as either Bluetooth or 802.11b type interference. Note that the interferer can be set to have a different carrier frequency and a random phase offset.

The IEEE 802.11b standard describes four modulation methods providing bit rates of 1, 2, 5.5, and 11 Mbits/sec [3]. The first rate is achieved by differential BPSK (DBPSK) with DSSS using an 11 chip Barker code; the chip rate is 11 Mchips/sec. The last rate is obtained using complementary code keying (CCK), also at

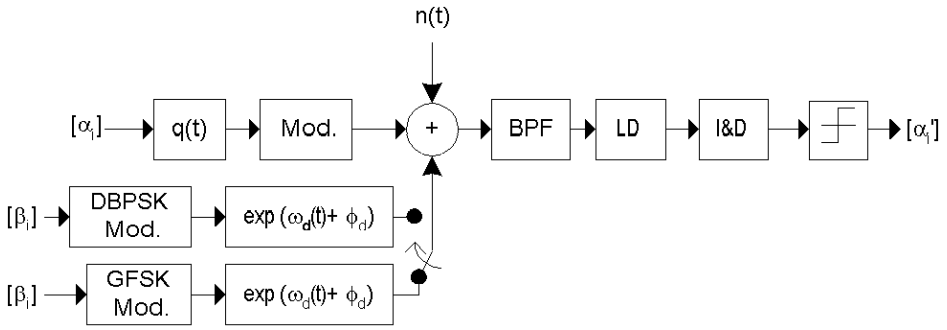

Figure 1: Bluetooth system model.

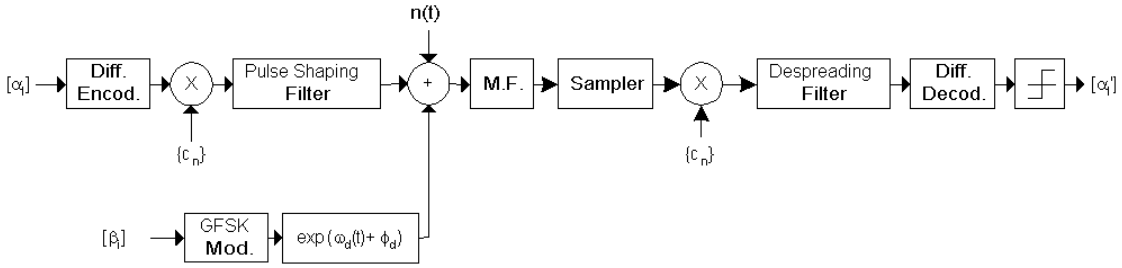

Figure 2: 802.11b DSSS system model.

11 Mchips/sec. In this study, we consider the 1 and 11 Mbits/sec bit rates. The communications system model for the 1 Mbit/sec bit rate is presented in Fig. 2, again consisting of the transmitter, the channel noise, the receiver and the Bluetooth interference source. We explain the details of this model in the following sections.

2 Bluetooth System Model

2-1 The GFSK signal

The GFSK signal can be represented by [4]

$$s(t, \mathbf{a}) = A\cos(2\pi f_c t + \phi(t, \mathbf{a})), \qquad (1)$$

where $A = \sqrt{\frac{2E_b}{T}}$, E_b is the energy per data bit, and f_c is the carrier frequency. $\mathbf{a}$ is the random input stream, comprised of the data bits α_i; $\phi(t, \mathbf{a})$ is the output phase deviation, given by

$$\phi(t, \mathbf{a}) = 2\pi h_f \int_{-\infty}^{t} \sum_{i=-\infty}^{n} \alpha_i g(\tau - iT) d\tau. \qquad (2)$$

One of the key ideas in GFSK is that a single bit is transmitted over multiple symbols, which is done by using a pulse shaping filter with impulse response $g(t)$ given by

$$g(t) = \frac{1}{2T}[Q(2\pi B_b \frac{t - \frac{T}{2}}{\sqrt{ln2}}) - Q(2\pi B_b \frac{t + \frac{T}{2}}{\sqrt{ln2}})], \qquad (3)$$

where $Q(t)$ is the standard Q-function $Q(t) = \int_t^\infty \frac{1}{\sqrt{2\pi}} e^{-\tau^2/2}$. By introducing controlled intersymbol interference, the spectral occupancy of the signal is substantially reduced.

Eq. (2) can also be written as

$$\phi(t, \mathbf{a}) = 2\pi h_f \sum_{i=n-L+1}^{n} \alpha_i q(t - iT) + \pi h_f \sum_{i=-\infty}^{n-L} \alpha_i, \qquad (4)$$

where L is the length of $g(t)$, and

$$q(t) = \int_{-\infty}^{t} g(\tau) d\tau. \qquad (5)$$

For Bluetooth with $B_b T = 0.5$, we have $L = 2$, which means that a single data bit is spread over two consecutive symbol intervals.

2-2 Channel Model

Recent measurements in the ISM band show that the root-mean-square (rms) average of the excess delay for the multipath component is around 30 nsec in an office environment [5, 6]. In another study, Kim *et al.* [7] found that the rms values were below 70 nsec, with an average value of approximately 50 nsec. For a line-of-sight (LOS) path, the power spectral density of the faded amplitude is close to a Rician distribution [7]. Therefore, we chose a flat fading channel model with a Rician distribution. This model assumes that a direct path exists between the transmitter and the receiver, and there are also other low-level scattered paths. The probability density function (pdf) of the Rician distribution is

$$P_R(r) = \frac{r}{\sigma^2} e^{-\frac{-r^2+\nu^2}{2\sigma^2}} I_0(\frac{r\nu}{\sigma^2}) \; r \geq 0, \qquad (6)$$

where I_0 is the zeroth-order modified Bessel function of the first kind, ν is the envelope of the strong component, and σ^2 is proportional to the power of the "scattered" Rayleigh component.

The Rician factor K is the ratio of the power in the direct path P_S to the power in the diffuse path P_d,

$$K = \frac{P_S}{P_d}. \qquad (7)$$

As K approaches zero, the channel behaves as Raleigh fading, whereas as K goes to infinity, the channel is Gaussian.

Two important parameters associated with the receiver are the average carrier-to-noise ratio $\overline{CNR}$, and the average carrier-to-interference ratio $\overline{CIR}$ defined as

$$\overline{CIR} = \frac{P_S + P_d}{P_I}, \qquad \overline{CNR} = \frac{P_S + P_d}{P_n}; \qquad (8)$$

P_I is the interference power, while P_n is the noise power in the receiver's frequency band.

In this simulation, we first consider the AWGN channel model, and then we apply the Rician fading. Also, because of the static behavior of the indoor channels, the Doppler shift frequency is ignored.

2-3 Interference Model

Either a Bluetooth or an 802.11b interference signal can be represented as

$$S_I(t, \mathbf{b}) = B\cos(2\pi(f_c + f_d)t + \phi_2(t, \mathbf{b})), \qquad (9)$$

where $\mathbf{b}$ is the random input data, which is independent of $\mathbf{a}$, and ϕ_2 depends on the type of the interferer. f_d is the frequency difference between the desired signal and the interference. The Bluetooth radio channels are 1 MHz apart, so f_d can take values of $0, 1, 2 \cdots$ MHz. The bandwidth of the 802.11b system is 22 MHz, so we carried out simulations for $f_d \leq 11$ MHz. The sampling rate is $N_s = 44$ samples/bit, which equals 4 samples/chip for the 802.11 DSSS system. This sampling rate is appropriate for f_d up to 22 MHz.

When studying interference, we want to reduce the effects of the traffic patterns and concentrate on the effects of time/frequency overlap between the two systems. For Bluetooth performance, we make these two assumptions: (1.) that the 802.11b WLAN is constantly transmitting and (2.) that any other Bluetooth piconets are synchronized to packet boundaries and are also transmitting. These correspond, in some sense, to worst case scenarios. In a real system, there will be times when the interferer is off. For the 802.11b system, we assume that the Bluetooth interferer is also always transmitting.

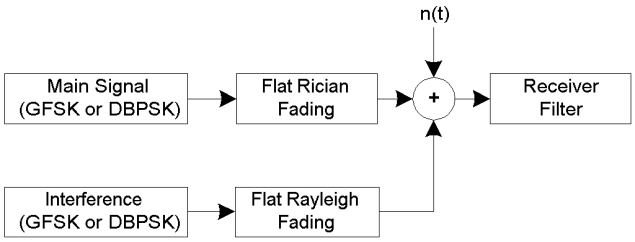

Figure 3: Interference model for the fading channels.

In the AWGN channel, a uniform random delay $t_d \in [0,\ T)$ and a random phase $\phi_d \in [0,\ 2\pi)$ are applied to the interferer signal for each packet. For the fading channels, it is assumed that the intended signal is subjected to Rician fading, whereas the interference undergoes Rayleigh fading. Fig. 3 shows a block diagram of this configuration. We chose $K = 5$ ($K \simeq 7$ dB) for

the desired signal, which is close to the profile recommended in [7].

2-4 LDI Receiver

This receiver consists of a pre-detection bandpass filter, a limiter-discriminator, and an integrate and dump filter, as shown in Fig. 1. The final block is the hard limiter, which compares the output phase with a decision level. The pre-detection bandpass filter is a Gaussian filter with an equivalent lowpass impulse response, $h_r(t)$, given by [8]

$$h_r(t) = \sqrt{\frac{2\pi}{ln2}} B_r \, e^{-(\frac{2\pi^2}{ln2})(B_r t)^2}, \qquad (10)$$

where B_r is the 3 dB bandwidth. According to Simon and Wang [8], the optimum bandwidth for this filter is $B_{IF} = 2B_r = 1.1/T$. The discrete impulse response of this filter is obtained by sampling and truncating $h_r(t)$.

The output of the receiver pre-detection filter can be represented using its inphase and quadrature components, $X(t)$ and $Y(t)$, respectively, as

$$\begin{aligned} e(t) &= X(t)\cos(2\pi f_c t) - Y(t)\sin(2\pi f_c t) \\ &= R(t)\cos[2\pi f_c t + \psi(t)]. \end{aligned} \qquad (11)$$

The limiter-discriminator output is thus

$$\psi'(t) = \frac{d\psi(t)}{dt} = \frac{X(t)Y'(t) - X'(t)Y(t)}{X^2(t) + Y^2(t)}. \qquad (12)$$

The discrete impulse response of an ideal differentiator is [9]

$$h_{diff}[n] = \frac{\cos(\pi(n - \frac{M}{2}))}{(n - \frac{M}{2})} - \frac{\sin(\pi(n - \frac{M}{2}))}{(n - \frac{M}{2})^2}. \qquad (13)$$

We truncate this impulse response using a Kaiser window with $M = 5$ and $\beta = 2.4$, and then we use it to approximate the derivatives of the quadrature components required in computing Eq. (12). Another approach to implement this filter is to use a simple difference equation.

The integrate-and-dump filter is simply a rectangular filter with impulse response

$$h_{ID}(t) = \begin{cases} \frac{1}{T} & 0 \le t < T \\ 0 & \text{otherwise.} \end{cases} \qquad (14)$$

The discrete-time filter is obtained by sampling $h_{ID}(t)$. The amplitude of the filter were normalized to 1. The appropriate sampling time for the system is chosen at the maximum eye opening.

3 802.11b System Model

3-1 1 Mbit/sec DSSS

The basic 1 Mbit/sec rate is encoded using DBPSK; thus, it is not necessary to have a coherent phase reference in the receiver to demodulate the received signal.

This system utilizes a spread spectrum scheme to mitigate the effect of a jammer. The Barker sequence with code length $P = 11$ is employed to spread the signal. The bit duration, T, is exactly 11 chip periods, T_c, long. The processing gain (PG) of this system is [10] $PG = \frac{R_c}{R_b} = 11$, where $R_b = \frac{1}{T}$ is the bit rate, and $R_c = \frac{1}{T_c}$ is the chip rate. If we calculate the power spectrum of the Barker codes, we get [11]

$$\begin{aligned} S(f) &= \sum_{\substack{k=-\infty \\ k \neq 0}}^{\infty} (\frac{P+1}{P^2}) sinc^2(\frac{k}{P}) \delta(f - \frac{k}{PT_c}) \\ &\quad + \frac{1}{P^2}\delta(f). \end{aligned} \qquad (15)$$

The function, $S(f)$, is illustrated in Fig. 4 for $P = 11$. We see that a narrowband interference signal -like Bluetooth- located at the middle of the spectrum will be more attenuated than an interferer located 1 MHz away from the middle of the spectrum.

As shown in Fig. 2, the input data bits are first differentially encoded. The resulting sequence is spread by the Barker code. The output of the spreader is fed to a Square-Root Raised-Cosine (SR-RC) pulse-shaping filter. The impulse response of the SR-RC filter with a roll-off factor α is [11]

$$\begin{aligned} p(t) &= \frac{sin[(1-\alpha)\pi t/T_c]}{(\pi t/T_c)[1 - (4\alpha t/T_c)^2]} \\ &\quad + \frac{4\alpha(t/T_c)cos[(1+\alpha)\pi t/T_c]}{(\pi t/T_c)[1 - (4\alpha t/T_c)^2]}. \end{aligned} \qquad (16)$$

The discrete time impulse response of this filter is obtained by sampling $p(t)$.

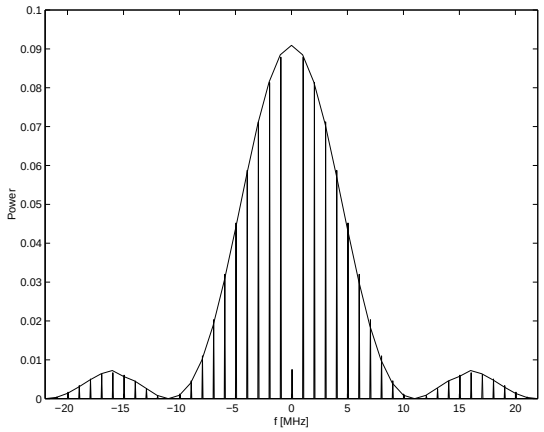

Figure 4: Power Spectrum of the Barker Code.

At the receiver, the input samples are first passed through the SR-RC matched filter. The despreading filter is a rectangular filter that integrates the output of the multiplier during a bit period. The differential decoder compares the phase angle of the received symbol and the previous one to generate the output bit stream. It is assumed that the chip timing of the receiver is synchronized to the transmitter.

3-2 11 Mbits/sec CCK

Complementary codes were originally conceived by M. J. Golay for infrared multislit spectrometry [12]. These codes can be considered block codes over the field of complex numbers. Let the kth code word be given by $\mathbf{s}_k = [s_{k1}\, s_{k2} \cdots s_{kN}]^T$, where N is the length of the code word, and $k = 1, 2, \cdots, K$. The autocorrelation of the code word is given by [13]

$$R_{kk}[j] = \sum_{i=1}^{N-j} s_{ki}\, s^*_{k(i+j)}. \qquad (17)$$

A set of K codes is considered complementary if and only if it satisfies the following equation

$$\sum_{k=1}^{K} R_{kk}[j] = \begin{cases} 0 & \text{for } j \neq 0 \\ KN & \text{for } j = 0. \end{cases} \qquad (18)$$

The complementary codes in the 802.11b standards are defined by a set of 256 8-chip code words. They are specified by

$$\begin{aligned} c = [&e^{j(\phi_1+\phi_2+\phi_3+\phi_4)}, \quad e^{j(\phi_1+\phi_3+\phi_4)}, \\ &e^{j(\phi_1+\phi_2+\phi_4)}, \quad -e^{j(\phi_1+\phi_4)}, \\ &e^{j(\phi_1+\phi_2+\phi_3)}, \quad e^{j(\phi_1+\phi_3)}, \\ &-e^{j(\phi_1+\phi_2)}, \quad e^{j(\phi_1)}], \end{aligned} \qquad (19)$$

where

$$\phi_i \in \{0, \frac{\pi}{2}, \pi, \frac{3\pi}{2}\} \quad \text{for } i = 1, 2, 3, 4. \qquad (20)$$

Note that each element of a code word is complex, and so can be transmitted using QPSK modulation as discussed below.

At 11 Mbits/sec, 8 bits (d0 to d7; d0 first in time) are transmitted per code word. The first dibit (d0, d1) encodes ϕ_1 based on DQPSK, which provides the possibility of employing differentially-coherent detection. In this study, we employ a coherent receiver, assuming that the initial phase of the signal is known. The dibits, (d2, d3), (d4, d5), and (d6, d7) encode ϕ_2, ϕ_3, and ϕ_4, respectively, as specified in Table 1.

Dibit Pattern (d_i, d_{i+1})	Phase
00	0
01	$\frac{\pi}{2}$
10	π
11	$\frac{3\pi}{2}$

Table 1: QPSK Encoding.

The system model is presented in Fig. 5. Only an AWGN channel is considered in this case.

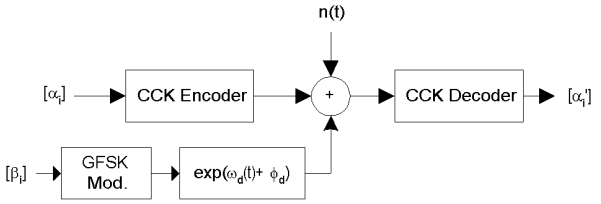

Figure 5: CCK System Model.

The decoder determines the valid code word that is closest to the received signal, and it maps that code word back to data bits. It is well known that in an AWGN channel, a code set which has the largest minimum Euclidean distance between code words yields the lowest bit error rate. Thus, an optimal code set for an AWGN channel would maximize the following minimum distance

$$\begin{aligned} d_{min} &= \min \|\mathbf{s}_k - \mathbf{s}_l\|^2 \\ k, l &\in \{1, 2, \cdots, K\}. \end{aligned} \qquad (21)$$

For complementary codes with length N and M possible phases, it can be shown that the minimum Euclidean distance is equal to [14]

$$d_{min} = \sqrt{\frac{N}{2} \| 1 - exp(j\frac{2\pi}{M}) \|}. \qquad (22)$$

For CCK with $N = 8$ and $M = 4$, the minimum distance is 2.82, which is 3 dB better than the distance of uncoded QPSK whose $d_{min} = 1.4$.

The maximum likelihood method described above needs a bank of 256 correlators in the receiver. Although optimum, this method may be considered too complex for some implementations. There are also less complex sub-optimum algorithms. By looking at the code words of CCK, one can write these equations for the decoded phases [14]

$$\begin{aligned} \phi_2 &= arg\{r_1 r_2^* + r_3 r_4^* + r_5 r_6^* + r_7 r_8^*\} \qquad (23) \\ \phi_3 &= arg\{r_1 r_3^* + r_2 r_4^* + r_5 r_7^* + r_6 r_8^*\} \\ \phi_4 &= arg\{r_1 r_5^* + r_2 r_6^* + r_3 r_7^* + r_4 r_8^*\} \\ \phi_1 &= arg\{r_4 e^{-j\phi_4} + r_6 e^{-j\phi_3} + r_7 e^{-j\phi_2} + r_8\}, \end{aligned}$$

where

$$\mathbf{r} = [r_1, r_2, r_3, r_4, r_5, r_6, r_7, r_8] \qquad (24)$$

is the received vector. We employ the above sub-optimal receiver to measure the performance in the presence of interference.

4 Link Budget

For a transmitter at a power level of P_T, the extracted power by the receiver's antenna may be expressed in decibels as

$$P_R = P_T + G_T + G_R - L_p - L_a, \qquad (25)$$

where G_T and G_R are the antenna gains of the transmitter and the receiver, respectively, L_p is the path loss, and L_a accounts for any additional system loss. For an indoor channel, we apply a simple propagation model: line-of-sight propagation (free space) for the first 8 m, thereafter a propagation exponent of 3.3. The path loss can be expressed as [15]

$$L_p = \begin{cases} 40 + 20 \log(d) & \text{for } d < 8 \text{ m} \\ 58.3 + 33 \log(d/8) & \text{for } d \geq 8 \text{ m}. \end{cases} \qquad (26)$$

Assuming 0 dB gain for the transmitter and the receiver antennas and ignoring additional loss, Eq. (26) can be written as

$$P_R = P_T - L_p. \qquad (27)$$

The sensitivity of the receiver, R_{sens}, which is the minimum amount of signal power required to achieve a certain bit error rate (BER), may be expressed as

$$R_{sens} = P_n + CNR_{req}. \qquad (28)$$

Here, P_n is the receiver noise power and CNR_{req} is the required carrier-to-noise ratio to achieve a $BER = 10^{-3}$ in an AWGN channel. The CNR is defined as

$$CNR = \frac{E_b}{N_0} \frac{1}{BT}. \qquad (29)$$

For Bluetooth, our simulation shows that at $CNR \simeq 16$ dB, we get a $BER = 10^{-3}$. Also, R_{sens} may be typically selected as R_{sens}=−80 dbm. By inserting these values, the receiver noise is then

$$P_n = R_{sens} - CNR_{req.} = \text{-96 dBm}. \qquad (30)$$

Using Eq. (27) and given P_n, we can calculate Bluetooth's CNR and CIR values for a chosen topology. Table 2 shows the CNR values for $P_T = 1$ mW.

Distance [m]	1	3	5	10	15
CNR [dB]	56	46	42	35	29

Table 2: CNR values for Bluetooth.

The above calculations can be repeated for the 802.11b receiver assuming $R_{sens} = -80$ dBm, and $CNR_{req} = 8$ dB at $BER = 10^{-3}$. Table 3 contains the results for $P_T = 25$ mW.

Distance [m]	1	3	5	10	15
CNR [dB]	62	52	48	40	35

Table 3: CNR values for 802.11b.

For distances less than 15 meters, the CNR is high enough so the errors are mainly caused by the interference signal.

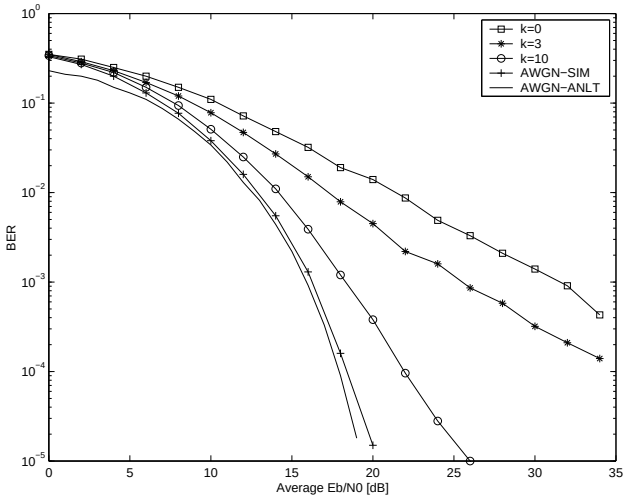

Figure 6: Bluetooth performance in the AWGN and Rician fading channels. LDI receiver.

5 Performance Results

5-1 Bluetooth

Simulation results for the LDI receiver in the AWGN and Rician channels are presented in Fig. 6. We see that for the AWGN case at $E_b/N_0 = 16$ dB, the $BER = 10^{-3}$. For the worst case Rayleigh fading condition ($K = 0$), an $E_b/N_0 = 30$ dB is required for the same BER. Also in this figure, we present the analytical BER curve using the method described in [16, 8] for the AWGN case.

Interference Type	Ratio (dB)
$C/I_{co-channel}$	11
C/I_{1MHZ}	0
C/I_{2MHZ}	-30
$C/I_{\geq 3MHZ}$	-40

Table 4: Specified CIR values for Bluetooth interference.

For Bluetooth interference on a Bluetooth signal, there is a specific requirement according to the standard, *i.e.* the BER shall be less than 0.1% in any of the conditions given in Table 4. The performance is measured with the desired signal 10 dB over the reference sensitivity level. Fig. 7(a) shows the performance in this case. We observe that the LDI receiver can meet the requirement set by the standard. Fig. 7(b) presents the performance with Bluetooth co-channel interference

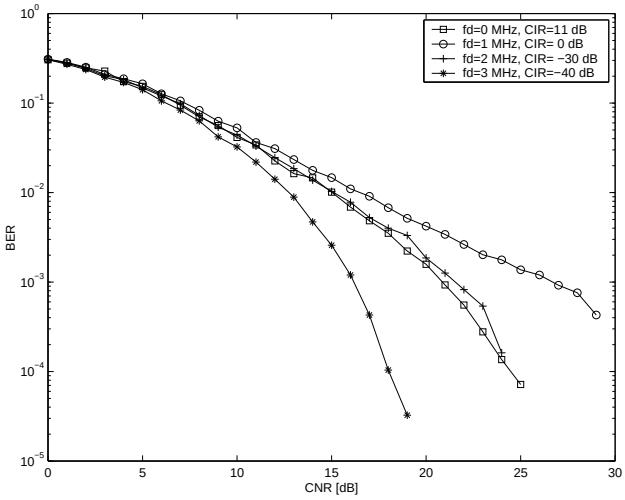

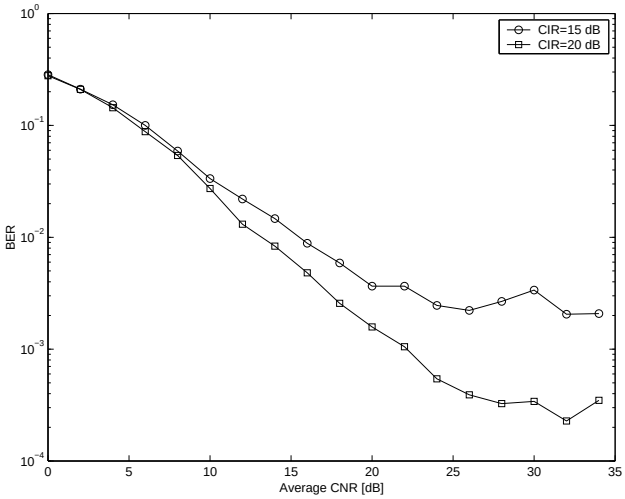

Figure 7: $\boxed{\frac{(a)}{(b)}}$ Bluetooth performance with Bluetooth interference. (a) AWGN channel. (b) Rician channel. LDI receiver.

in the Rician fading channel. As mentioned in Section 2-3, $K = 5$ for the signal, and $K = 0$ (Rayleigh) for the interference. The $\overline{CIR}$ value should be at least 20 dB in order to get low BER for the co-channel interference.

Next, we study the performance of Bluetooth with 802.11b interference. The curves in Figs. 8(a) and (b) are for an interference-limited environment with $CNR = 30$ dB. The 802.11b signal looks like broadband noise at the input to the Bluetooth receiver. The performance degradation for carrier frequency differences up to 4 MHz is almost the same, and so we plot the results for $f_d = 0$ as a representative case. The null in the Barker code spectrum does not improve the performance here, but it does for the

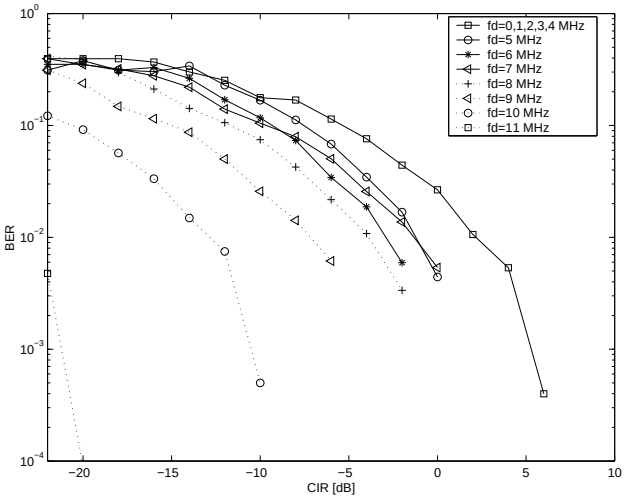

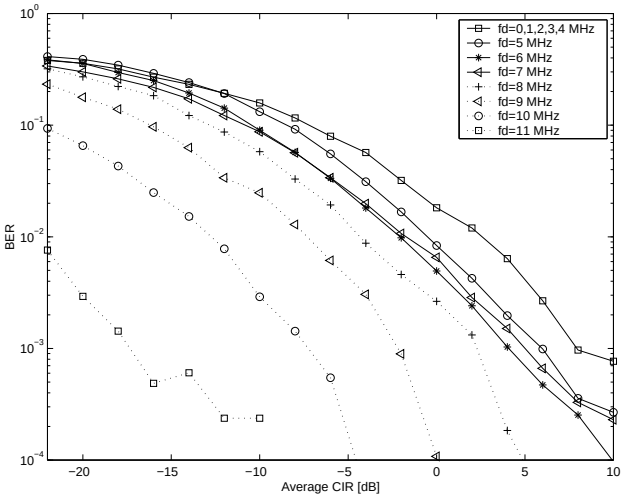

Figure 8: $\boxed{\frac{(a)}{(b)}}$ Bluetooth performance with 802.11b interference. (a) AWGN channel. (b) Rician channel. LDI receiver.

802.11b DSSS system. After 4 MHz, one gradually sees the effect of the pulse shaping filter of the 802.11b transmitter, which has a null at $f_d = 11$ MHz. In fact, the CIR value at $f_d = 11$ MHz has to be very low in order to cause high BER.

To relate the CIR values to the transmitter powers, consider the topology where the Bluetooth transmitter and the 802.11b interference are both positioned one meter away from the Bluetooth receiver; the Bluetooth transmitter power is 1 mW, while the 802.11b's is 25 mW. Using Eq. (27), $CIR \simeq -14$ dB. So, when a Bluetooth packet hops on a frequency that is less than 10 MHz away from the center of the 802.11 interference, that packet is usually subjected to errors. The roll-off factor α of the 802.11b transmitter determines the range of frequency offsets over which high BERs are observed. In this simulation, we chose $\alpha = 1$, so the interference signal will occupy the maximum available bandwidth. Another observation from Fig. 8(a) is that if the CIR value is always greater than 6 dB, the BER for all frequency offsets is less than 10^{-3}.

The performance in the Rician channel ($K = 5$ for the signal and $K = 0$ for the interference) is shown in Fig. 8(b). We see that $\overline{CIR} = 10$ dB is the minimum tolerable. In comparison to scenarios where the desired signal undergoes Rayleigh fading or the interference has a LOS path, these results may be considered optimistic. On the other hand, we see that since the interference acts as wideband noise, there is not a great difference in the CIR requirement between the AWGN and Rician channel models.

As a solution to mitigate the effect of interference, we use a simple two-state Viterbi receiver for Bluetooth. Again, we assume that the phase of the transmitted signal is known to the receiver. The performances for Bluetooth and for 802.11 interferences are shown in Figs. 9(a) and (b), respectively. A dramatic enhancement is observed in these figures, evidently at a cost of having a more complicated receiver. This improvement is particularly considerable for 802.11b interference, which acts as broadband noise in the Bluetooth receiver's bandwidth.

5-2 802.11b

Now, we consider the performance of the 1 Mbit/sec 802.11b system, again in an interference-limited environment with $CNR = 35$ dB. Since the system takes advantage of DSSS, one observes in Fig. 10(a) that for co-channel interference, $CIR = -11$ dB is adequate to suppress the effect of interference ($BER \leq 10^{-2}$). The most disturbing interference is located at $f_d = 1$ MHz, which needs a minimum CIR of -5 dB. This difference stems from the null at the middle of the spectrum of the Barker code as described before. For frequency offsets grater than 8 MHz, the CIR value must be very low in order to get a high BER. This fact is due

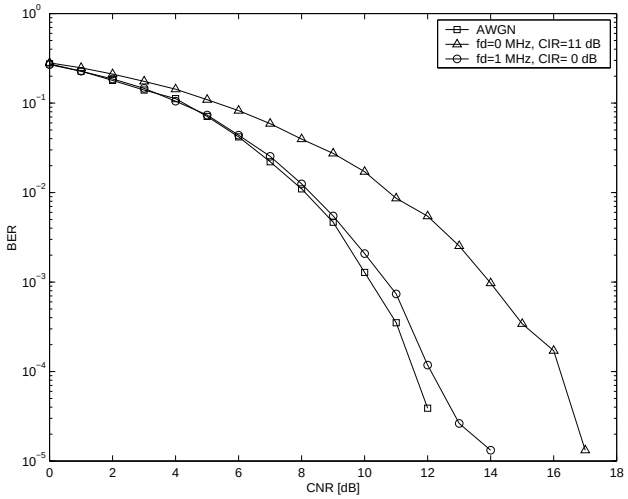

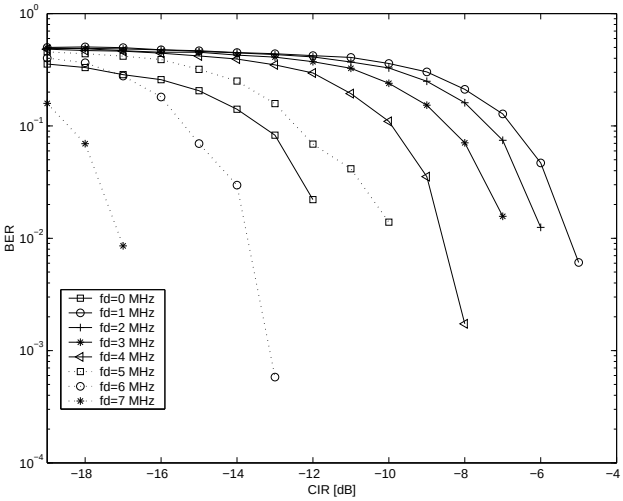

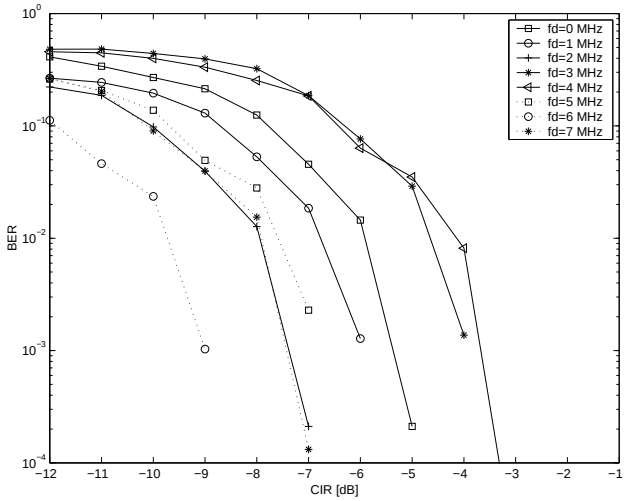

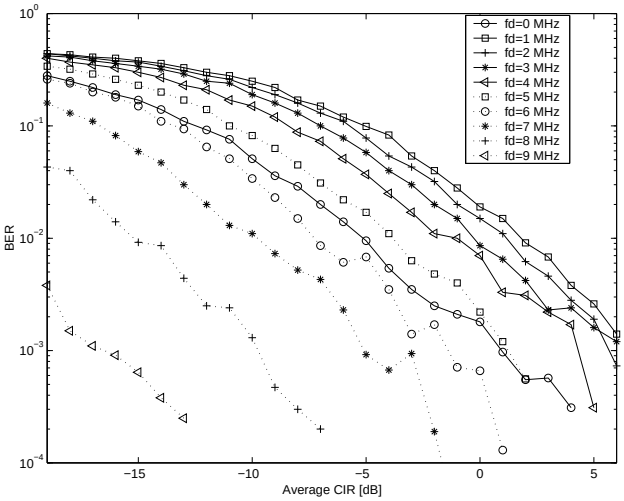

Figure 9: $\boxed{\frac{(a)}{(b)}}$ Bluetooth Viterbi receiver performance. (a) Bluetooth interference. (b) 802.11b interference. AWGN channel.

Figure 10: $\boxed{\frac{(a)}{(b)}}$ 802.11b DSSS performance with Bluetooth interference. (a) AWGN channel. (b) Rician channel.

to the bandpass filter in the 802.11b receiver having high attenuation at frequencies near 11 MHz. The results of this figure are comparable to the analytic method proposed in [17, 18].

Fig. 10(b) indicates the performance in the Rician channel ($K = 5$), where the Bluetooth interference is subjected to Rayleigh fading. The minimum $\overline{CIR}$ in this case is $\overline{CIR} = 2$ dB ($BER = 10^{-2}$). For the 802.11b DSSS system, there is a difference of 7 dB in CIR required to achieve acceptable performance in AWGN and Rician channels, respectively. This difference is greater than the equivalent (4 dB) for the Bluetooth system, using the LDI receiver.

Fig. 11(a) shows the performance of the 11 Mbits/sec 802.11b CCK receiver in the AWGN channel. The optimum receiver performs about 2 dB better than QPSK, and the sub-optimum method is nearly the same as QPSK. The sub-optimal system provides a BER of 10^{-3} for an $E_b/N_o = 8$ dB. It must be noted that CCK was designed explicitly for fading channels, where its gain over QPSK is much more significant.

Fig. 11(b) illustrates the performance of 11 Mbits/sec IEEE 802.11b receiver with Bluetooth interference. This figure indicates that the CCK modulation is more vulnerable to the interference signal than the 1 Mbits/sec DSSS. A minimum CIR of 3 dB must be achieved to get $BER = 10^{-2}$ for all frequency offsets. This result is not surprising, since the CCK provides a higher bit rate but occupies the same 22 MHz

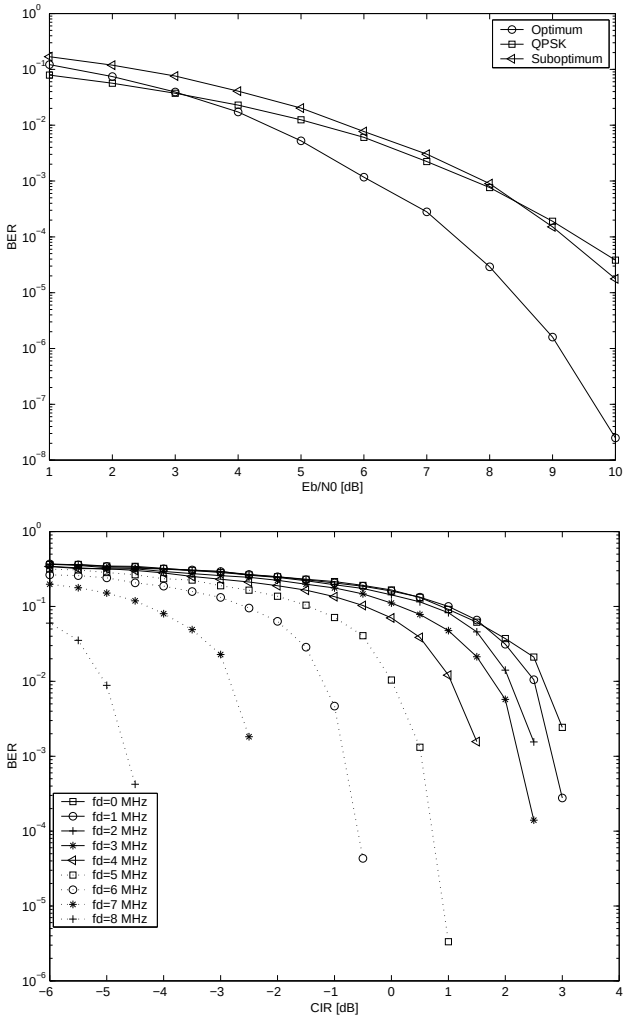

Figure 11: $\boxed{\frac{(a)}{(b)}}$ 802.11b CCK performance. (a) AWGN channel. (b) Bluetooth interference.

bandwidth, thereby having less of a coding gain. Generally, the receivers used for both 1 Mbit/sec and 11 Mbits/sec are fairly simple, and improved performance can most likely be obtained using more complicated signal processing. This fact is especially true for the 11 Mbits/sec CCK system.

6 Conclusions and Present Work

In this work, we have investigated the performance of Bluetooth and 802.11b WLANs in interference-limited environments. We have established preliminary performance results for both the AWGN and fading channel models. The simulations strongly suggest that the interference may severely damage the operation of both systems in some applications. The AWGN results for the effect of interference on Bluetooth are not very far from the fading results, so this model may be adequate for studying the effect of interference in LOS conditions. Moreover, the AWGN channel can be used to evaluate mechanisms designed to improve coexistence.

While most of the study used the simple LDI receiver for Bluetooth, the simulation results suggest that substantially better performance can be achieved using a coherent Viterbi receiver for interference-limited channels. Presently, we are developing a more sophisticated Viterbi receiver, including channel estimation based on the Bluetooth access code.

For the 802.11b DSSS receiver, the results in a fading channel are more degraded than in an AWGN channel, compared to Bluetooth. Therefore, coexistence studies need to chose a more realistic channel model, instead of assuming an AWGN one. Furthermore, multipath fading is even more of a concern for the 11 Mbits/s CCK system, given its relatively short symbol time. Thus, a RAKE-based CCK receiver, which exploits the frequency-selective properties of the channel, should probably be used.

This paper considers the physical layer of the Bluetooth and 802.11b systems, including the design of the radio receivers. However, it does not consider the medium access control (MAC) layer. In Bluetooth, this layer contains the forward error detection and correction, the automatic repeat request (ARQ) protocols, and the frequency hopping. For 802.11b, the MAC is more complex, containing carrier sense, multiple access with collision avoidance, as well as a number of other features. Our current goal is to determine the interference-limited performance of the combined physical and MAC layers for each system with realistic traffic and topologies. Metrics of interest include packet loss probabilities, number of residual errors in a packet, delay, and throughput.

7 Acknowledgment

The authors wish to thank Dr. L. E. Miller for his helpful comments during the course of this study.

References

[1] J. C. Haartsen and S. Mattisson, "Bluetooth - A new low-power radio interface providing short-range connectivity," *Proc. of the IEEE*, vol. 88, no. 10, pp. 1651-1661, Oct. 2000.

[2] Bluetooth Special Interest Group, *Specifications of the Bluetooth System, vol. 1, v.1.0B*, Dec. 1999. Available : http:/www.bluetooth.com.

[3] IEEE Std. 802-11, *IEEE Standard for Wireless LAN Medium Access Control (MAC) and Physical Layer (PHY) Specification*, 2001 Edition.

[4] R. Steele (Ed.), *Mobile Radio Communications*, John Wiley & Sons Inc., 1996.

[5] G. J. M. Janssen, P. A. Stigter and R. Prasad, "Wideband indoor channel measurements and BER analysis of frequency selective multipath channels at 2.4, 4.75, and 11.5 GHz," *IEEE Trans. Comm.*, pp. 1272-1288, Oct. 1996.

[6] H. J. Zepernick and T. A. Wysocki, "Multipath channel parameters for the indoor radio at 2.4 GHz ISM band," *49th IEEE Veh. Tech. Conf.*, vol. 1, pp. 190-193, 1999.

[7] S. C. Kim, H. L. Bertoni and M. Stern, "Pulse propagation characteristics at 2.4 GHz inside buildings," *IEEE Trans. Veh. Tech.*, vol. 45, pp. 579-592, Aug. 1996.

[8] M. K. Simon and C. C. Wang, "Differential detection of Gaussian MSK in a mobile radio environment, " *IEEE Trans. Veh. Tech.*, pp. 307-320, Nov. 1984.

[9] A. L. Oppenheim and R. W. Schafer, *Discrete-Time Signal processing*, Prentice Hall, 1989.

[10] J. G. Proakis, *Digital Communications*, McGraw-Hill, 1995.

[11] J. S. Lee and L. E. Miller, *CDMA Engineering Handbook*, Artech House, 1998.

[12] M. J. E. Golay,"Complementary series," *IRE Trans. Information Theory*, vol. IT-7, pp. 82-87, Apr. 1961.

[13] S. Halford, K. Halford and M. Webster, "Complementary code keying for RAKE-based indoor wireless communications," *IEEE Int. Conf. on Circuits and Systems*, pp. 427-430, May 1999.

[14] R. D. J. Van Nee, "OFDM codes for peak-to-average power reduction and error correction," *IEEE Global Telecommun. Conf.*, London vol. 1, pp. 740-744, Nov. 1996.

[15] A. Kamerman, "Coexistence between Bluetooth and IEEE 802.11 CCK solutions to avoid mutual interference interference," *Lucent Technologies Bell Laboratories technical report*, Jan. 1999

[16] M. K. Simon and C. C. Wang, "Differential versus limiter discriminator detection of narrow-band FM," *IEEE Trans. Comm.*, pp. 1227-1234, Nov. 1983.

[17] D. L. Schilling, L. B. Milstein, R. L. Pickholtz and R. W. Brown, "Optimization of the processing gain of an M-ary direct sequence spread spectrum communication system," *IEEE Trans. Comm.*, pp. 1389-1398, Aug. 1980.

[18] L. B. Milstein, S. Davidovici, and D. L. Schilling, "The effect of multiple-tone interfering signals on a direct sequence spread spectrum communication system," *IEEE Trans. Comm.*, vol. 30, pp. 436-446, Mar. 1982.